Notch3 Promotes Prostate Cancer-Induced Bone Osteoblastic Metastasis in an MMP-3-Dependent Manner

Sourik S. Ganguly[1], Galen Hostetter[2], Lin Tang[3], Sander B. Frank[1,3], Kathylynn Saboda[4], Rohit Mehra[5], Lisha Wang[5], Xiaohong Li[1], Evan T. Keller[5], and Cindy K. Miranti[3,*]

[1]Program for Skeletal Disease and Tumor Microenvironment, Center for Cancer and Cell Biology, and [2]Tissue Repository and Pathology Core, Van Andel Research Institute, Grand Rapids, MI, USA; [3]Department of Cellular and Molecular Medicine, University of Arizona Cancer Center, and [4]Department of Epidemiology, University of Arizona, Tucson, AZ, USA; [5]Department of Pathology, University of Michigan, Ann Arbor, MI, USA

Running Title: Notch3 and MMP-3 in bone metastasis

Key Words: prostate cancer bone metastasis, notch, MMP, osteoblasts, osteoclasts

Word Count: 4982

* Corresponding Author:

Cindy K Miranti

University of Arizona Cancer Center

1515 N. Campbell Ave

Tucson, AZ 85718

Cmiranti@email.arizona.edu

520-626-2269

ABSTRACT

Purpose: Over ninety percent of prostate cancer metastasis is localized in the bone where it induces a unique osteoblastic response. Elevated Notch signaling is associated with advanced high-grade disease and metastasis, but how it contributes to osteoblastic bone metastasis is unknown.

Experimental Design: To determine how Notch affects prostate cancer bone metastasis, Notch expression was manipulated in mouse tibia xenografts and tumor growth, lesion phenotype, and tumor microenvironment assessed. Patient bone metastases were assessed for Notch3 and MMP-3 expression.

Results: Osteoblastic tumor cells expressed 5-6 times more Notch3, than osteolytic tumor cells. Expression of active Notch3 (NICD3) in osteolytic tumors reduced osteolytic lesion area and enhanced osteoblastogenesis, while loss of Notch3 in osteoblastic tumors enhanced osteolytic lesion area and decreased osteoblastogenesis. This was accompanied by a respective decrease and increase in number of active osteoclasts at the tumor-bone interface, without any effect on tumor proliferation. Conditioned medium from NICD3-expressing cells enhanced osteoblast differentiation and proliferation in vitro, while simultaneously inhibiting osteoclastogenesis. MMP-3 was specifically elevated in NICD3-expressing tumors, and inhibition of MMP-3 rescued the NICD3-induced block in osteolytic lesions, suppressed osteoblast proliferation, and stimulated osteoclastogenesis. Human bone metastasis samples had higher levels of Notch3 and MMP-3 compared to patient matched visceral metastases.

Conclusions: We identified a Notch3-MMP-3 axis in human prostate cancer bone metastases that promotes osteoblastic lesion formation by blocking osteoclast differentiation, while stimulating osteoblastogenesis. This newly identified Notch3-MMP-3 axis could be used as a therapeutic target for inhibiting osteoblastic bone metastasis.

CLINICAL RELEVANCE

Prostate cancer-induced bone metastasis is incurable as patients ultimately develop resistance to current therapies. Prostate cancer interaction with the bone microenvironment uniquely favors osteoblastic lesion development. The mechanisms that promote osteoblastic metastasis are not fully understood and this information is required to develop better therapeutic approaches. We identified Notch3-dependent induction and secretion of MMP-3 as new axis in prostate cancer bone metastases. Notch3 and MMP-3 are co-upregulated in human prostate cancer bone metastases, where they promote osteoblastic lesions by suppressing osteoclast differentiation and enhancing osteoblastogenesis. This study provides evidence, for the first time, of a newly identified Notch3-MMP-3 axis that promotes prostate cancer-induced lesion development, which could be used as a therapeutic target for inhibiting osteoblastic bone metastasis.

INTRODUCTION

Prostate cancer is the most common non-skin cancer in males, and second leading cause of mortality, with death primarily due to metastasis (1, 2). Prostate cancer invariably metastasizes to the bone and forms osteoblastic (bone-forming) lesions. Such lesions cause severe bone pain, fractures, bone deformity, hypercalcemia, and immunological complications (1, 3). Even though prostate cancer metastasis is typically osteoblastic, markers of bone turnover indicate that underlying osteolytic events are also involved (4, 5). Death from metastatic bone disease is due in part to the lack of effective therapy, the development of which requires knowing the mechanisms that control this mixed blastic/lytic phenotype.

Bone, a dynamic connective tissue, is constantly remodeling during an individual's lifetime. Remodeling depends on two cells types, osteoblasts and osteoclasts, both of which work in harmony to maintain normal bone. Osteoblasts, derived from mesenchymal stem cells, make new bone. Osteoclasts, derived from monocytes, degrade bone. During osteoblastic metastasis, the bone remodeling balance favors bone formation, i.e. osteoblastogenesis (1, 6).

Notch, known for its role in development and tissue differentiation, is also involved in cancer progression and metastasis. There are four single-pass transmembrane Notch receptors in mammals, activated by five different transmembrane ligands (JAG1/2 and DLL1/3/4) from adjacent cells upon cell-cell contact. Upon ligand binding, Notch is first cleaved by ADAM10 and then by γ-secretase to release the Notch intracellular cytoplasmic domain (NICD). NICD translocates to the nucleus and forms a transcription activation complex by associating with the proteins CBF-1, Suppressor of Hairless, Lag2, and Mastermind-like (MAML). This complex activates the transcription of Notch target genes like Hairy enhancer of split (Hes) and Hes-related YRPF motif (Hes) transcription factors (7-9). Majority of the studies investigating normal prostate gland development and prostate cancer have focused on Notch1. In the normal prostate, Notch1 is required for basal cell maintenance, luminal progenitor proliferation, and branching morphogenesis (10, 11). In prostate cancer, knockdown of Notch1

inhibits invasion, decreases growth, suppresses colony formation *in vitro*, and increases chemosensitivity (12, 13). Elevated Notch1 staining is observed in aggressive prostate tumors relative to prostatic intraepithelial neoplasia and normal tissue (12). These data suggest Notch1 may be a driver of prostate cancer progression.

Recent studies demonstrate that Notch3 is also involved in normal prostate development where it is required for luminal cell differentiation (11, 14, 15). Furthermore, elevated Notch3 expression positively correlates with prostate cancer progression, recurrence, and drug resistance (16-20). In metastatic breast cancer, Jag-1 in tumor cells activates Notch signaling in osteoblasts to stimulate osteoclastogenesis in osteolytic bone lesions, while Notch3 is induced in tumor cells by osteoblasts (21, 22). However, the role of Notch3 in cancer cells and its influence on osteolytic versus osteoblastic disease remains unknown.

Matrix metalloproteinases (MMPs) are a family of proteases secreted by stromal and tumor cells whose expression is a prerequisite for tumor progression. MMPs are increased in many cancers and negatively correlated with patient survival (23). MMP-1, 3, 7 and 9 reportedly promote prostate cancer metastasis to the bone (5). Both MMP mRNA and protein are elevated in serum and tissue samples from prostate cancer patients and is correlated with advanced and metastatic disease (23). Polymorphisms in MMP-3 predict for increased prostate cancer risk and MMP-3 levels are elevated specifically in patients with bone metastases (24, 25). MMP-1, 9, and 13 are required for bone resorption, and MMP-9 promotes osteoclast polarization and ruffled border formation (5). Although Notch1 reportedly promotes the expression of MMP-9 (12), it is unknown whether Notch3 contributes to the expression of MMPs or which ones.

During our studies, we observed elevated Notch3 expression in human prostate cancer bone metastases and hypothesized that Notch3 promotes bone metastasis by remodeling the bone microenvironment. Herein, we report that Notch3 contributes to osteoblastic bone metastasis by suppressing osteoclasts and stimulating osteoblastogenesis through induction of MMP-3.

MATERIALS AND METHODS

Cells lines and animals

PC3 and 22Rv1 cells were obtained from ATCC, and C4-2B cells was obtained from Dr. Robert Sikes (University of Delaware) (26). All lines were maintained in RPMI1640 (Gibco) supplemented with 10%FBS (Gemini). All lines were validated by STR analysis and periodically checked for mycoplasma contamination using MycoAlert PLUS kit (Lonza). Conditioned medium was collected by starving sub-confluent cells for 24 h in α-MEM (Gibco).

The 5-6 week old male NSG mice used in this study were bred and maintained in a pathogen-free and ALAAC-certified barrier facility following guidelines from VARI Institutional Animal Care and Use Committee and the Department of Defense (DOD) Animal Care and Use Committee.

Doxycycline-inducible shRNA and NICD

Doxycycline-inducible shRNA targeting Notch3 was generated as previously described (14, 27). Doxycycline-inducible NICD1 was PCR subcloned from EF.hICN1.CMV.GFP into pENTR3C (Invitrogen) between SalI and NotI sites, creating pENTR3C-NICD1, using the following primers: Fwd 5'- AATTGTCGACCCAAGCTGGCTAGTTAAGC-3', Rev 5'-TTAAGCGGCCGCTTTATTCCAGCACACTGGCGGC-3'. EF.hICN1.CMV.GFP was a gift from Linzhao Chen (Addgene plasmid #17623) (28). Cloned inserts were amplified with Syzygy SyFi high fidelity polymerase (Integrated Scientific Solutions, SY-100) and ligated with LigateIT rapid ligase (Affymetrix). Doxycycline inducible NICD3 was PCR subcloned from pCLE-NICD3 into pENTR3C between SalI and NotI, creating pENTR3C-NICD3, using primers:

Fwd 5'-AATTGTCGACCCCGCCTCTAGCACTTTGG-3',

Rev 5'-TTAAGCGGCCGCTTTATTCGATCTAAGAACTGACGAGCG-3'.

pCLE-NICD3 was a gift from Nicholas Gaiano (Addgene plasmid #26894) (29). pENTR3C-NICD1 and pENTR3C-NICD3 were recombined via L/R Clonase II (Thermo) into pLenti-CMV-Puro-DEST (w118-1) to make pLenti-Tet-NICD1-Puro and pLenti-Tet-NICD3-Puro.

pLenti-CMV-Puro-DEST (w118-1) was a gift from Eric Campeau and Paul Kaufman (Addgene plasmid #17452) (30). Integrity of all the plasmids was verified by Sanger sequencing.

PC3 cells were first infected with pLenti-CMV-TetR-Blast (716-1). pLenti-CMV-TetR-Blast (716-1) was a gift from Eric Campaeau and Paul Kaufmann (Addgene plasmid #17492) (30) and a stable pooled TetR line was created by selecting in 2 µg/ml blasticidin. TetR line was infected with NICD1 or NICD3-expressing lentivirus and pooled clones selected in 2 µg/ml puromycin. Cell lines targeting MMP-3 with shRNA were generated by purchasing a lentiviral shRNA knockdown vector containing MMP-3 shRNA sequence (pLV[shRNA]-Hygro-U6>hMMP3) from Vector Builder. Targeting sequence was 5'-AGAGTAACAGCTGGCTTAATT-3'. Pooled cell lines were generated by selecting in 20 µg/ml hygromycin. Doxycycline (200-500 ng/ml) (Sigma) was used to induce expression of Notch shRNAs, NICD1, or NICD3 in *in vitro* cultured cell lines.

Mouse injections and radiographic imaging

One million PC3 or C4-2B cells or 0.2 x 10^6 22Rv1 cells were resuspended in 10 µl of PBS and injected into the tibiae of 5-6 week old male NSG mice. As a control, 10 µl of PBS was injected into the contralateral tibia. Each experiment had a minimum of 7, and up to 12, mice per cohort. Half the mice injected with Notch3 shRNA, NICD1, or NICD3 expressing cells were provided with 1 mg/ml Doxycycline in the drinking water supplemented with 5% Sucrose (Millipore) starting from the 1st day of injection and changed weekly. Control mice received only 5% sucrose. Mice were radiographically imaged weekly using Bioptics piXarray Digital Specimen Radiography (Faxitron Bioptics). The lytic bone lesions were scored in a blinded manner by measuring the area of all visible lesions using MetaMorph quantitative image analysis software (Molecular Devices, Inc.). At the end-point of the study (~3-4 weeks for PC3, ~8 weeks for C4-2B and 22Rv1), tibiae were snap frozen for RNA and protein analysis or fixed in formalin for immunohistochemistry (IHC).

For subcutaneous injections, 1.0 x 10^6 PC3, C4-2B, or 22Rv1 cells resuspended in 100 µl of PBS were injected subcutaneously into the flank area of 5 to 6 week old male NSG mice and tumors harvested after 4 or 8 weeks and frozen in liquid nitrogen.

Bone marrow differentiation and proliferation assays

Mouse bone marrow cells were extracted from the long bones of 5 to 6 week old naïve NSG mice, plated in α-MEM medium supplemented with 10%FBS, left to adhere for 3 d, and then differentiated into osteoblasts using 50 µg/ml Vitamin C for another 7 d. The medium was changed every 3 d. On the third day of culture, bone marrow cells were treated with conditioned medium from prostate cancer cell lines bearing Tet-inducible Notch3 shRNA or NICD3 plasmids treated with or without doxycycline. On the last 3 days, the medium was changed to serum-starved medium. Alkaline phosphatase (ALP) staining were performed by fixing cells in 10% neutral buffered formalin and then staining cells using NBT/BCIP Substrate Solution (Thermo Scientific) at 37^0C. Osteoblast colony formation was monitored by staining duplicate wells with 0.5% crystal violet.

For osteoclastogenesis, the bone marrow cells were plated in α-MEM supplemented with 10% FBS. After 24 hours, unattached cells were replated and cultured in α-MEM supplemented with 10% FBS and 25 ng/ml macrophage colony-stimulating factor (mCSF). Two days later cells were supplemented with 25 ng/ml mCSF and 30 ng/ml RANKL (R&D) for another 4 d. For the last 4 days, cells were treated with conditioned medium from prostate cancer cell lines bearing Tet-inducible Notch3 shRNA or NICD3 plasmids treated with or without doxycycline. Medium was changed to serum-starved medium for the last 24 h of culture. TRAP staining was performed according to manufactures protocol (Sigma Aldrich). TRAP-positive multinucleate (2 $\geq$ nuclei/cell) osteoclasts were counted in 10 random fields under 20x magnification.

Osteoblast proliferation was evaluated via MTT assay with cells plated in triplicate using the manufacturers protocol (ATCC). In a subset of assays, cultured osteoblasts or osteoclasts were treated with recombinant human MMP-3 (Abcam).

Histology and immunohistochemistry

Mouse tibiae were harvested and fixed in 10% neutral-buffered formalin (Sigma) for 4 d at 4 °C, followed by decalcification in 14% EDTA for 5-6 d at 4 °C, and then embedded in paraffin. Serial bone sections 5 µm thick were used for lHC staining. Hematoxylin and eosin (H&E) and TRAP staining were done as previously reported (31). Paraffin embedded sections were stained using antibodies against Ki67 (1:100; Thermo Scientific; RM-9106), MMP-3 (1:100; Abcam; ab52915), or Notch3 (1:300; Santa Cruz; sc5593).

TRAP and Ki67 quantification

Serial sections stained for TRAP were scanned and images collected using Aperio software. TRAP-positive multinucleate osteoclasts (2 $\geq$ nuclei/cell) at the bone/tumor interface were counted at 20X magnification. Ki67 was quantified by counting three-four random fields under 40X magnification. All counting was blinded.

TMA staining and quantification

Tissue microarray (TMA) sections having patient-matched visceral and bone metastasis from 30 patients was obtained from the Prostate Cancer Bioreprisotory Network (PCBN), warm-autopsy program, UWTMA79. The TMA-170 microarray, consisting of patient-matched visceral and bone metastasis from 10 patients, was prepared from tissues obtained from the rapid autopsy program at University of Michigan. Both TMAs were stained using MMP-3 (1:75, Abcam; ab52915) and Notch3 (1:1000; Protein Tech 55114-1-AP) antibodies. Two board-certified pathologists without any prior knowledge of the patients' clinical information independently used H and modified H scoring to quantify the TMAs for MMP-3 and Notch3 expression.

Protein extraction, immunoblot, ELISA, and cytokine array

Mouse tibiae and subcutaneous tumors were snap-frozen in liquid nitrogen. Frozen tibiae were homogenized in RIPA buffer (32) using a FastPrep-24 tissue homogenizer (MP Biomedicals). Prostate cancer cell lines were lysed using RIPA buffer as described previously

(32). Total protein (10-20 µg) was separated by SDS-PAGE and transferred to PVDF membranes (Fisher). Membranes were blocked with 5% BSA-TBST and incubated with antibodies diluted in 5% BSA-TBST as previously described (32). Primary antibodies were detected using HRP-conjugated secondary antibodies (Sigma) by chemiluminescence using Quantity One imaging software on a Bio-Rad Gel Docking system. Antibodies listed in Supplementary Table S1.

Equal amounts of protein from subcutaneous or tibiae tumors pooled from two mice were incubated with a 174 protein spotted human cytokine antibody array C2000 (Ray Biotech Inc) according to the manufacturer's protocol.

MMP-3 ELISA (R&D) was performed on 24 h serum-starved PC3-NICD3 cells treated with or without doxycycline. Media were collected and concentrated (Ultracel-10k;Millipore) and equal amounts were used to quantify total MMP-3.

RNA extraction and qRT-PCR

Total RNA was extracted from frozen tibiae or cell lines using TRIzol (Invitrogen, Carlsbad, CA). Equal amounts of RNA were reverse transcribed through the SuperScript first-strand synthesis system (Invitrogen) and qRT-PCR was performed using SYBR Green Supermix (Bio-Rad, Hercules, CA) on Applied BioSystems. Primers were synthesized by Integrated DNA Technologies (IDT, Coralville, IA) and the levels of target mRNAs were standardized to GAPDH and plotted as Log_2-fold. Primers listed in Supplementary Table S2.

Statistical analysis

All statistical analysis on the mice with one or two comparison groups used Student's *t*-test and in experiments where more than two groups were being compared, ANOVA was used. In all statistical analyses the two-tailed significance is reported. For biostatistical analysis of the TMAs, multivariate analysis of Notch3 and MMP3 expression levels in visceral versus bone metastases was conducted using mixed effect models. The mixed effect models accounted for the correlation between the measurements obtained across multiple observations per

individuals. Spearman correlation was used to calculate correlation between MMP-3 and Notch3 expression across all tissues.

RESULTS

Notch3 inhibits osteolytic bone lesion development.

Prostate cancer cells, which promote osteolytic (PC3) or mixed (blastic/lytic) lesions (C4-2B and 22Rv1), were assayed for Notch1 and Notch3 expression by qRT-PCR and immunoblotting. Both Notch1 and Notch3 mRNAs were higher in the osteoblastic lines, C4-2B and 22Rv1, relative to the lytic PC3 cells (Fig. 1A-B). Notch3 mRNA expression was 2-3-fold higher than Notch1. Notch1 and Notch3 protein paralleled the increase in mRNA (Fig.1C-D). Thus, Notch might play a role in osteoblastic lesion development.

Osteolytic PC3 cells were engineered to express doxycycline-inducible Notch3 intracellular domain, NICD3. PC3-NICD3 cells were injected into mouse tibiae and mice fed sucrose as controls or doxycycline to induce NICD3 expression. Radiographic imaging after 3 weeks showed the expected osteolytic lesion development in control PC3-NICD3-injected tibiae (Fig. 1E). Induction of NICD3 by doxycycline significantly reduced osteolytic lesion area (Fig 1E). H&E staining validated tumor growth in the bone, and IHC staining confirmed NICD3 induction in the doxycycline-treated tumors (Fig. 1F).

PC3 cells engineered to induce NICD1, did not produce any significant changes in osteolytic lesion area when injected tibial tumors were stimulated with doxycycline (Supplementary Fig. S1A). The observed changes in lesion area were not due to non-specific effects of doxycycline, as doxycycline treatment of mice injected with non-NICD expressing tumors did not alter osteolytic lesion formation (Supplementary Fig. S1B). Thus, specific induction of NICD3, but not NICD1, reduces osteolytic lesion formation in prostate tumors in the bone.

To determine whether the decrease in osteolytic lesion development by NICD3 was due

to changes in tumor proliferation, we monitored Ki67 expression by IHC staining. There was no difference in proliferation between PC3 control and PC3 NICD3-expressing tumors (Supplementary Fig. S2A). To assess the effects of Notch3 on the bone microenvironment, we quantified the number of TRAP-positive osteoclasts. There was over a 2-fold decrease in the number of TRAP-positive osteoclasts at the tumor-bone interface in doxycycline-treated PC3-NICD3 tumors compared to sucrose-treated tumors (Fig. 1F). Thus, the effect of NICD3 is on the tumor microenvironment, rather than an intrinsic effect on tumor growth.

Blocking Notch3 increases osteolytic lesions.

To determine if loss of Notch3 enhances osteolysis, we injected PC3 cells harboring doxycycline-inducible Notch3 shRNA (PC3-shN3) into mouse tibiae. PC3-shN3 doxycycline-treated tumors had significantly more lytic lesion area compared to sucrose-treated control tumors (Fig. 1G). Loss of Notch3 expression by doxycycline treatment was validated by IHC (Fig. 1H). There was no change in tumor proliferation (Supplementary Fig. S2B) and the doxycycline-treated PC3-shN3 tumors had significantly more TRAP positive cells (Fig. 1H).

To assess whether blocking Notch3 expression in osteoblastic tumors enhances lytic lesions, we injected 22Rv1 or C4-2B cells harboring doxycycline-inducible Notch3 shRNA into mouse tibiae. Loss of Notch3 in doxycycline-treated tumors significantly increased osteolytic lesion area over 2-fold (Fig. 2A). Loss of Notch3 expression was confirmed by IHC staining (Fig. 2B-C). Loss of Notch3 also resulted in a 2-fold increase in the number of osteoclasts at the tumor-bone interface (Fig. 2B-C). Loss of Notch3 had no effect on tumor cell proliferation (Supplementary Fig. S2C-D). Thus, expression of active Notch3 in prostate tumors in the bone inhibits osteolytic lesion development independent of tumor proliferation.

Notch3 induces the expression of MMP-3 in prostate cancer bone lesions.

To identify secreted factors that contribute specifically to osteoblastic bone lesion development, we used a human cytokine array to compare subcutaneous tumors versus tibial tumors generated from PC3, C4-2B, or 22Rv1 cells. MMP-3 was specifically elevated in C4-2B

and 22Rv1 bone tumors, compared to their subcutaneous tumors (Fig. 3A). No change in MMP-3 levels was observed between PC3 tumors in the bone versus skin.

To investigate whether Notch3 controls MMP-3 expression, PC3-NICD3, PC3-shN3, or C4-2B-shN3 tibial tumors were analyzed for MMP-3 expression by IHC and qRT-PCR. MMP-3 protein was elevated in the doxycycline-treated PC3-NICD3 tumors relative to sucrose-treated control tumors (Fig. 3B). Conversely, loss of Notch3 expression in PC3-shN3 or C4-2B-shN3 tumors by doxycycline reduced MMP-3 levels relative to controls (Fig. 3B). Human-specific MMP-3 mRNA was increased by doxycycline in PC3-NICD3 tumors (Fig. 3C), and decreased by Notch3 loss in PC3-shN3 and C42B-shN3 tumors (Fig. 3D-E). Furthermore, induction of NICD3 in PC3-NICD3 cells induced the secretion of MMP-3 into the conditioned medium (Fig. 3F). These results indicate Notch3 induces the expression of MMP-3.

Notch3 in cancer cells changes osteoblast and osteoclast differentiation.

There are two ways in which NICD3, acting in tumor cells, could inhibit osteolytic lesions: through a decrease in osteoclastogenesis or through an increase in osteoblastogenesis. To evaluate these possibilities, we analyzed expression of osteoclast inhibitors in PC3-NICD3 tumor-bearing tibiae. Mouse-specific IL-10 mRNA, an inhibitor of osteoclastogenesis (33, 34), is upregulated over 8-fold in doxycycline-treated PC3-NICD3 tumors relative to sucrose-treated controls (Fig. 4A). In addition, the ratio of mouse-specific OPG/RANKL mRNA is elevated over 2-fold in PC3-NICD3 tibiae (Fig. 4B), which limits osteoclastogenesis (35). This increase in osteoclastogenesis inhbitors by NICD3 *in vivo* supports the decrease in TRAP staining (i.e. active osteoclasts) seen around the NICD3-expressing tumors (see Fig. 1F). Conversely, there was a corresponding significant 5-8-fold increase in osteoblast markers, bone sialoprotein (BSP), osteocalcin (OCN), and alkaline phosphatase (ALP) (Fig 4C), in the doxycycline-treated PC3-NICD3 tumors. Thus, NICD3 expression in tumors leads to both increased osteoblastogenesis and decreased osteoclastogenesis.

To more directly measure the effect of the NICD3-expressing tumor cells on osteoblasts,

conditioned medium (CM) from doxycycline-treated PC3-NICD3 cells was added to differentiating osteoblasts *in vitro*. CM from doxycycline-stimulated PC3-NICD3 cells enhanced osteoblast differentiation as measured by increased alkaline phosphatase (ALP) staining and increased colony formation (Fig. 4D). This was accompanied by a 3- to 4-fold increase in osteoblast differentiation markers, i.e. Osterix (OSX), BSP, and OCN (Fig. 4E). CM from doxycycline-treated PC3-NICD3 cells also stimulated osteoblast proliferation (Fig. 4F) and expression of Cyclin A, D and E (Fig. 4G).

To investigate how Notch3 expression in cancer cells affects osteoclasts, we added CM from doxycycline-treated PC3-NICD3 cells to differentiating osteoclasts. NICD3 CM inhibited the formation of active osteoclasts as measured by the reduced number of fused multinucleated TRAP-positive cells (Fig. 4H) and reduced mRNA expression of late osteoclast differentiation markers, particularly the calcitonin receptor (Fig. 4I). Reciprocally, CM from doxycycline-treated C4-2B-shN3 or 22Rv1-shN3 cells stimulated the formation of TRAP-positive multinucleate osteoclasts (Fig. 4J-K). Finally, CM from doxycycline-treated C4-2B-NICD3 cells decreased the number of TRAP-positive multinucleate osteoclasts (Fig. 4L). We did not observe any effects of the CM on osteoclast survival; CM did not induce caspase3 cleave as assessed by immunostaining (not shown). Together these results indicate that CM from Notch3-expressing cells inhibits osteoclast differentiation while simultaneously stimulating osteoblast proliferation and differentiation, leading to a net increase in blastogenesis in Notch3-expressing tumors.

Notch3 inhibits osteolytic bone lesion development in an MMP3-dependent manner.

To determine if Notch3 induction of MMP-3 is responsible for the observed effects of NICD3-CM on osteoblasts and osteoclasts, we directly tested the ability of human recombinant MMP-3 (rMMP3) to regulate differentiation. The addition of rMMP3 to differentiating osteoclasts reduced the formation of TRAP-positive multinucleate cells (Fig. 5A), but had no effect on osteoblast differentiation as measured by ALP staining (Fig. 5B). However, rMMP3 did promote osteoblast proliferation (Fig. 5C).

To investigate the dependency of NICD3 on MMP-3 for its inhibitory effects on osteoclasts, PC3-NICD3 cells were engineered to stably express MMP-3 shRNA (shMMP3). CM from doxycycline-treated PC3-NICD3-shMMP3 cells rescued the block in TRAP-positive multinucleate cell differentiation induced by CM from doxycycline-treated PC3-NICD3 cells (Fig. 5D) and prevented the promotion of osteoblast proliferation (Fig. 5E). We tested whether MMP-3 shRNA could also rescue osteolytic lesion formation. Doxycycline-treated PC3-NICD3-shMMP3 tibial tumors had increased osteolytic lesion area relative to doxycycline-treated PC3-NICD3 (Fig. 5F). MMP-3 knock-down and NICD3 induction was validated by IHC staining of tibial tumors (Fig. 5G). While tumor proliferation was decreased ~20% in the PC3-NICD3-shMMP3 tumors relative to PC3-NICD3 tumors, this was independent of NICD3 or shMMP3 expression (Supplementary Fig. S2E). Thus, rescue of the osteolytic phenotype occurs independent of tumor proliferation. Altogether, these data indicate MMP-3 is required for Notch3-mediated inhibition of osteolytic bone lesion development by prostate tumors.

Notch3 and MMP-3 are upregulated in human bone metastatic prostate cancer

Notch signaling pathway components are upregulated in Gleason 8 compared to Gleason 6 tumors (17). Furthermore, expression of Notch3 in prostate tumors is inversely correlated with patient survival (36), indicating the likely importance of Notch3 in prostate cancer progression. To measure the level of Notch3 and MMP-3 in prostate cancer bone metastases, two human tissue microarrays, TMA-170 with 10 matched primary, visceral, and bone metastases, and UWTMA79 with 30 matched visceral and bone metastases, were analyzed by IHC with antibodies to Notch3 or MMP-3. Bone metastases expressed more Notch3 and MMP-3 compared to matched patient visceral metastases (Fig. 6A,B). Furthermore, there was a significant correlation between expression of Notch3 and MMP-3 in all metastases (Fig. 6C). Altogether, our findings indicate that a Notch3-MMP-3 axis plays an integral part in prostate cancer osteoblastic bone metastasis.

DISCUSSION

Our studies demonstrate that Notch3 activation in prostate cancer bone metastases suppresses osteolytic lesions through induction and secretion of MMP-3, which acts to suppress osteoclast differentiation and enhance osteoblast proliferation. Notch3 expression increases with Gleason grade, suggesting its importance in cancer progression (18). Notch3 is also associated with prostate cancer recurrence (16). This is the first study to demonstrate that Notch3 is highly expressed in human prostate cancer bone metastases. Interestingly, Notch3 is activated by hypoxia, and bone metastases are highly hypoxic (18, 37). The hypoxic bone environment could be the driver of elevated Notch3 expression.

The promotion of osteoblast proliferation and differentiation by simply inducing NICD3 expression in an osteolytic cell line, suggests Notch3 is a key regulator of the osteoblastic phenotype that is so unique to prostate cancer. While prostate cancer is highly osteoblastic, there are also underlying osteolytic events (4, 5, 38). Our findings indicate that elevated Notch3 reduces the osteolytic events through its extrinsic effects on the bone microenvironment, with little to no intrinsic effect on tumor cell proliferation. NICD3 accomplishes this by promoting osteoblastogenesis while simultaneously inhibiting osteoclastogenesis; thus, tipping bone remodeling towards enhanced bone formation. We further found that this osteolytic suppression is MMP3-dependent. MMP-3 is known to promote the cleavage of PTHrP produced by cancer cells, which stimulates osteoblast migration and mineralization *in vitro* but lacks the osteolytic function associated with full length PTHrP (39). PTHrP also promotes osteoblast proliferation (40). Thus, the effects of the Notch3-MMP-3 axis on osteoblasts might depend in part on MMP-3-cleaved PTHrP. A previous study demonstrated that MMP-3 induces osteoclast death (41); however, we did not detect induction of any caspase-dependent cell death in our in vitro cultures either from NICD3-conditioned medium or by recombinant MMP-3.

This is the first study to demonstrate how MMP-3, secreted from cancer cells, modulates the function of bone cells in prostate cancer bone lesions. MMP-3 expression is higher in

primary human prostate tumors compared to PIN and normal tissue (42), and MMP-3 was previously reported to be elevated in a prostate cancer bone xenograft, but the source or function was not identified (43). MMP-3 is highly expressed in other cancers like breast, lung, pancreas, and osteocarcome, which correlates with poor patient survival (44, 45). We are the first to demonstrate elevated MMP-3 expression in human bone metastases, compared to visceral metastases, in prostate cancer patients. Furthermore, Notch3 expression is similarly elevated in bone metastases and correlates with elevated MMP-3 expression.

MMP-3 expression is induced in osteoblasts in response to inflammatory signals or mechanical stress and is necessary for bone remodeling (46, 47). Thus, tumors that secret MMP-3 may access this normal bone stress response. Interestingly, MMP-3 is elevated in the serum of rheumatoid arthritis patients, which is accompanied by both bone remodeling and inflammation (48). MMP-3 levels are reportedly higher in the serum of prostate cancer patients with bone metastatic disease (24). Our data provide mechanistic evidence and clinical relevance of a Notch3-MMP3 axis in prostate cancer osteoblastic bone metastasis.

In the past ten years there have been improvements in the options to treat bone metastatic prostate cancer; however, the available drugs (docetaxel, carbitaxel, abiraterone or enzalutamide) only increase patient survival for a short time as most patients eventually develop resistance to these drugs and finally succumb to the disease (1, 49). Our data demonstrates that NICD3 modulates the bone microenvironment, but has minimal effects on tumor cell proliferation. This suggests that inhibitors of Notch alone might not be effective at reducing tumor burden. Furthermore, while inhibition of Notch3 activity will decrease osteoblastic lesions, it may enhance lytic lesions by promoting osteoclast function and inhibiting the osteoblasts. Increasing the function of osteoclasts in osteoblastic metastasis could be an important step towards rebalancing bone homeostasis; however, there will be a need for combinatorial therapy to inhibit the excessive osteolysis caused by Notch inhibition. Bisphosphonates, which inhibit bone destruction by inhibiting osteoclast activity (5), could be used in combination with Notch3

inhibitors to rebalance bone homeostasis.

New γ-secretase inhibitors (pan-Notch inhibitors) in combination with bicalutamide have been in clinical trials but were terminated with no useful information (50). Recently, Cui et al demonstrated that a γ-secretase inhibitor in combination with docetaxel showed greater antitumor activity than either agent alone in DU145 prostate cancer tibial xenografts (20). Thus, to effectively reduce both tumor growth and block abnormal bone remodeling, it will be necessary to use combination treatments that target both the tumor and the tumor microenvironment.

Conflict of Interest:

The authors declare no conflict of interest.

ACKNOWLEDGEMENTS

Funding for this project was provided by a Postdoctoral Fellowship from DOD, W81XWH-16-1-0136 to support SSG. Additional funding was provided by the Van Andel Research Institute, University of Arizona, and University of Arizona Cancer Center (UACC) NCI/NIH P30CA023074. We wish to thank the following: Dr. Denise Roe, Director of Biostatistics Shared Resource at UACC for biostatistics support; Dr. Chunyan Liu at Ventana Medical Services, Oro Valley, AZ for her pathology services; Alexandra VanderArk, Veronique Schulz, and Ghada Y.T Mohsen for their technical expertise; Zachary Madaj for statistical analysis expertise; Lisa Turner of the VARI Pathology and Biorepository Core for her pathology expertise; Su Yanli and Staff of the VARI Vivarium and Transgenics core for technical assistance with animal experiments; David Nadziejka for technical editing of the manuscript; and Jeanie Wedberg for administrative support.

REFERENCES

1. Ganguly SS, Li X, and Miranti CK. The host microenvironment influences prostate cancer invasion, systemic spread, bone colonization, and osteoblastic metastasis. *Front Oncol.* 2014;4:364.
2. Siegel RL MK, Jemal A. Cancer statistics, 2015. *CA Cancer J Clin.* 2015;65(1):5-29.
3. Karayi MK, and Markham AF. Molecular biology of prostate cancer. *Prostate Cancer Prostatic Dis.* 2004;7(1):6-20.
4. Roudier MP, Morrissey C, True LD, Higano CS, Vessella RL, and Ott SM. Histopathological assessment of prostate cancer bone osteoblastic metastases. *J Urol.* 2008;180(3):1154-60.
5. Sottnik JL, and Keller ET. Understanding and targeting osteoclastic activity in prostate cancer bone metastases. *Curr Mol Med.* 2013;13(4):626-39.
6. Jin JK, Dayyani F, and Gallick GE. Steps in prostate cancer progression that lead to bone metastasis. *Int J Cancer.* 2011;128(11):2545-61.
7. Frank SB, and Miranti CK. Disruption of prostate epithelial differentiation pathways and prostate cancer development. *Front Oncol.* 2013;3:273.
8. Kopan R, and Ilagan MX. The canonical Notch signaling pathway: unfolding the activation mechanism. *Cell.* 2009;137(2):216-33.
9. Zanotti S, and Canalis E. Notch and the skeleton. *Mol Cell Biol.* 2010;30(4):886-96.
10. Wang XD, Shou J, Wong P, French DM, and Gao WQ. Notch1-expressing cells are indispensable for prostatic branching morphogenesis during development and re-growth following castration and androgen replacement. *J Biol Chem.* 2004;279(23):24733-44.
11. Kwon OJ, Valdez JM, Zhang L, Zhang B, Wei X, Su Q, Ittmann MM, Creighton CJ, and Xin L. Increased Notch signalling inhibits anoikis and stimulates proliferation of prostate luminal epithelial cells. *Nat Commun.* 2014;5(4416.

12. Bin Hafeez B, Adhami VM, Asim M, Siddiqui IA, Bhat KM, Zhong W, Saleem M, Din M, Setaluri V, and Mukhtar H. Targeted knockdown of Notch1 inhibits invasion of human prostate cancer cells concomitant with inhibition of matrix metalloproteinase-9 and urokinase plasminogen activator. *Clin Cancer Res.* 2009;15(2):452-9.

13. Ye QF, Zhang YC, Peng XQ, Long Z, Ming YZ, and He LY. Silencing Notch-1 induces apoptosis and increases the chemosensitivity of prostate cancer cells to docetaxel through Bcl-2 and Bax. *Oncol Lett.* 2012;3(4):879-84.

14. Frank SB, Berger PL, Ljungman M, and Miranti CK. Human prostate luminal cell differentiation requires NOTCH3 induction by p38-MAPK and MYC. *J Cell Sci.* 2017;130(11):1952-64.

15. Zhang S, Chung WC, Wu G, Egan SE, and Xu K. Tumor-suppressive activity of Lunatic Fringe in prostate through differential modulation of Notch receptor activation. *Neoplasia.* 2014;16(2):158-67.

16. Long Q, Johnson BA, Osunkoya AO, Lai YH, Zhou W, Abramovitz M, Xia M, Bouzyk MB, Nam RK, Sugar L, et al. Protein-coding and microRNA biomarkers of recurrence of prostate cancer following radical prostatectomy. *Am J Pathol.* 2011;179(1):46-54.

17. Ross AE, Marchionni L, Vuica-Ross M, Cheadle C, Fan J, Berman DM, and Schaeffer EM. Gene expression pathways of high grade localized prostate cancer. *Prostate.* 2011;71(14):1568-77.

18. Danza G, Di Serio C, Ambrosio MR, Sturli N, Lonetto G, Rosati F, Rocca BJ, Ventimiglia G, del Vecchio MT, Prudovsky I, et al. Notch3 is activated by chronic hypoxia and contributes to the progression of human prostate cancer. *Int J Cancer.* 2013;133(11):2577-86.

19. Cui J, Wang Y, Dong B, Qin L, Wang C, Zhou P, Wang X, Xu H, Xue W, Fang YX, et al. Pharmacological inhibition of the Notch pathway enhances the efficacy of androgen deprivation therapy for prostate cancer. *Int J Cancer.* 2018.

20. Cui D, Dai J, Keller JM, Mizokami A, Xia S, and Keller ET. Notch pathway inhibition using PF-03084014, a γ-secretase inhibitor (GSI), enhances the antitumor effect of docetaxel in prostate cancer. *Clin Cancer Res.* 2015;21(20):4619-29.

21. Zhang Z, Wang H, Ikeda S, Fahey F, Bielenberg D, Smits P, and Hauschka PV. Notch3 in human breast cancer cell lines regulates osteoblast-cancer cell interactions and osteolytic bone metastasis. *Am J Pathol.* 2010;177(3):1459-69.

22. Sethi N, Dai X, Winter CG, and Kang Y. Tumor-derived JAGGED1 promotes osteolytic bone metastasis of breast cancer by engaging notch signaling in bone cells. *Cancer Cell.* 2011;19(2):192-205.

23. Gong Y, Chippada-Venkata UD, and Oh WK. Roles of matrix metalloproteinases and their natural inhibitors in prostate cancer progression. *Cancers (Basel).* 2014;6(3):1298-327.

24. Srivastava P, Kapoor R, and Mittal RD. Impact of MMP-3 and TIMP-3 gene polymorphisms on prostate cancer susceptibility in North Indian cohort. *Gene.* 2013;530(2):273-7.

25. Jung K. NL, Lein M., Priem F., Schnorr D., Loening S.A. Matrix metalloproteinases 1 and 3, tissue inhibitor of metalloproteinase-1 and the complex of metalloproteinase-1/tissue inhibitor in plasma of patients with prostate cancer. *Int J Cancer.* 1997;74(220-3.

26. Thalmann GN, Sikes RA, Wu TT, Degeorges A, Chang SM, Ozen M, Pathak S, and Chung LW. LNCaP progression model of human prostate cancer: androgen-independence and osseous metastasis. *Prostate.* 2000;44(2):91-103 Jul 1;44(2).

27. Frank SB, Schulz VV, and Miranti CK. A streamlined method for the design and cloning of shRNAs into an optimized Dox-inducible lentiviral vector. *BMC Biotechnol.* 2017;17(1):24.

28. Yu X AJ, Chun JH, Friedman AD, Heimfeld S, Cheng L, Civin CI. HES1 inhibits cycling of hematopoietic progenitor cells via DNA binding. *Stem Cells.* 2006;24(4):876-88.

29. Dang L YK, Wang M, Gaiano N. Notch3 signaling promotes radial glial/progenitor character in the mammalian telencephalon. *Dev Neurosci.* 2006;28(1-2):58-69.

30. Campeau E RV, Rodier F, Smith CL, Rahmberg BL, Fuss JO, Campisi J, Yaswen P, Cooper PK, Kaufman PD. A versatile viral system for expression and depletion of proteins in mammalian cells. *PLoS One.* 2009;4(8):e6529.

31. Li X, Sterling JA, Fan KH, Vessella RL, Shyr Y, Hayward SW, Matrisian LM, and Bhowmick NA. Loss of TGF-beta responsiveness in prostate stromal cells alters chemokine levels and facilitates the development of mixed osteoblastic/osteolytic bone lesions. *Mol Cancer Res.* 2012;10(4):494-503.

32. Edick MJ, Tesfay L, Lamb LE, Knudsen BS, and Miranti CK. Inhibition of integrin-mediated crosstalk with epidermal growth factor receptor/Erk or Src signaling pathways in autophagic prostate epithelial cells induces caspase-independent death. *Mol Biol Cell.* 2007;18(7):2481-90.

33. Hong MH WH, Jin CH, Pike jw. The inhibitory effect of interleukin-10 on mouse osteoclast formation involves novel tyrosine-phosphorylated proteins. *J Bone Miner Res.* 2000;15(5):911-8.

34. Evans KE, and Fox SW. Interleukin-10 inhibits osteoclastogenesis by reducing NFATc1 expression and preventing its translocation to the nucleus. *BMC Cell Biol.* 2007;8:4.

35. Boyce BF, and Xing L. Biology of RANK, RANKL, and osteoprotegerin. *Arthritis Res Ther.* 2007;9 Suppl 1:S1.

36. Hudson RS, Yi M, Esposito D, Watkins SK, Hurwitz AA, Yfantis HG, Lee DH, Borin JF, Naslund MJ, Alexander RB, et al. MicroRNA-1 is a candidate tumor suppressor and prognostic marker in human prostate cancer. *Nucleic Acids Res.* 2012;40(8):3689-703.

37. Gilkes DM. Implications of Hypoxia in Breast Cancer Metastasis to Bone. *Int J Mol Sci.* 2016;17(10).

38. Keller ET, and Brown J. Prostate cancer bone metastases promote both osteolytic and osteoblastic activity. *J Cell Biochem.* 2004;91(4):718-29.

39. Frieling JS, Shay G, Izumi V, Aherne ST, Saul RG, Budzevich M, Koomen J, and Lynch CC. Matrix metalloproteinase processing of PTHrP yields a selective regulator of osteogenesis, PTHrP1-17. *Oncogene.* 2017;36(31):4498-507.

40. Ibrahim T, Flamini E, Mercatali L, Sacanna E, Serra P, and Amadori D. Pathogenesis of osteoblastic bone metastases from prostate cancer. *Cancer.* 2010;116(6):1406-18.

41. Garcia AJ, Tom C, Guemes M, Polanco G, Mayorga ME, Wend K, Miranda-Carboni GA, and Krum SA. ERalpha signaling regulates MMP3 expression to induce FasL cleavage and osteoclast apoptosis. *J Bone Miner Res.* 2013;28(2):283-90.

42. Furic L, Rong L, Larsson O, Koumakpayi IH, Yoshida K, Brueschke A, Petroulakis E, Robichaud N, Pollak M, Gaboury LA, et al. eIF4E phosphorylation promotes tumorigenesis and is associated with prostate cancer progression. *Proc Natl Acad Sci U S A.* 2010;107(32):14134-9.

43. Lynch CC, Hikosaka A, Acuff HB, Martin MD, Kawai N, Singh RK, Vargo-Gogola TC, Begtrup JL, Peterson TE, Fingleton B, et al. MMP-7 promotes prostate cancer-induced osteolysis via the solubilization of RANKL. *Cancer Cell.* 2005;7(5):485-96.

44. Christine Mehner EM, Aziza Nassar, William R. Bamlet, Evette S. Radisky and Derek C. Radisky. Tumor cell expression of MMP3 as a prognostic factor for poor survival in pancreatic, pulmonary, and mammary carcinoma. *Genes & Cancer.* 2015;6(480-9.

45. Jie-Feng Huang W-XD, Jun-Jie Chen. Elevated expression of matrix metalloproteinase-3 in human osteosarcoma and its association with tumor metastasis. *JBOUN.* 2016;21(1):235-43.

46. Sasaki K, Takagi M, Konttinen YT, Sasaki A, Tamaki Y, Ogino T, Santavirta S, and Salo J. Upregulation of matrix metalloproteinase (MMP)-1 and its activator MMP-3 of human osteoblast by uniaxial cyclic stimulation. *J Biomed Mater Res B Appl Biomater.* 2007;80(2):491-8.

47. Kusano K, Miyaura C, Inada M, Tamura T, Ito A, Nagase H, Kamoi K, and Suda T. Regulation of matrix metalloproteinases (MMP-2, -3, -9, and -13) by interleukin-1 and interleukin-6 in mouse calvaria: association of MMP induction with bone resorption. *Endocrinology.* 1998;139(3):1338-45.

48. Ally MM, Hodkinson B, Meyer PW, Musenge E, Tikly M, and Anderson R. Serum matrix metalloproteinase-3 in comparison with acute phase proteins as a marker of disease activity and radiographic damage in early rheumatoid arthritis. *Mediators Inflamm.* 2013;2013(183653.

49. Imamura Y, and Sadar MD. Androgen receptor targeted therapies in castration-resistant prostate cancer: Bench to clinic. *Int J Urol.* 2016;23(8):654-65.

50. Su Q, and Xin L. Notch signaling in prostate cancer: refining a therapeutic opportunity. *Histol Histopathol.* 2016;31(2):149-57.

Figure Legends

Figure 1. NICD3 inhibits osteolytic lesions. Levels of (**A**) Notch1 and (**B**) Notch3 mRNA in tumor cell lines. Log_2-fold change relative to PC3 cells. Levels of (**C**) Notch1 and (**D**) Notch3 measured by immunoblotting. Tubulin is loading control. (**E,G**) PC3 cells harboring Tet-inducible (**E**) NICD3 or (**G**) Notch3 shRNA (shN3) injected into tibiae of mice treated with sucrose (Suc) or doxycycline (Dox). X-rayed lytic lesion area quantified. (**F,H**) Tibiae were stained with H&E (top), anti-Notch3 (middle), TRAP (bottom), and number of osteoclasts quantified. T=tumor and B=bone; arrows indicate TRAP+ osteoclasts. Error bars are S.E.M, $n \geq 11$. *$0.01 \leq p < 0.05$; **$0.001 \leq p < 0.01$; ***$p < 0.001$

Figure 2. Inhibiting Notch3 promotes osteolytic lesions. (**A-B**) 22Rv1 or (**C**) C4-2B cells harboring doxycycline-induced Notch3 shRNA (shN3) injected into tibiae of mice treated with sucrose (Suc) or doxycycline (Dox). (**A**) X-rayed lytic lesion area quantified. **(B-C)** Tibiae were stained with H& E (top), anti-Notch3 (middle), TRAP (bottom), and number of osteoclasts quantified. T=tumor; B=bone; arrows indicate TRAP+ osteoclasts. Error bars are S.E.M, n=7. *$0.01 \leq p < 0.05$; **$0.001 \leq p < 0.01$; ***$p < 0.001$

Figure 3. Notch3 promotes the expression of MMP3. (**A**) PC3, 22Rv1, or C4-2B cells were injected subcutaneously or intra-tibially and tumor lysates applied to a cytokine array. Levels of MMP-3 signal shown. (**B**) Tibiae from mice injected with PC3-NICD3, PC3-shN3 (Notch3 shRNA), or C4-2B-shN3 cells treated with sucrose (Suc) or

doxycycline (Dox) were stained with human-specific MMP-3 antibody. T=tumor (**C-E**) Levels of human-specific MMP-3 mRNA from tibiae in (A) assessed by qRT-PCR. Expression is relative to sucrose. (**F**) Levels of MMP-3 in conditioned medium (CM) from PC3-NICD3 cells treated with vehicle (Ctrl) or doxycycline (Dox) assessed by ELISA. Error bars are S.E.M, $n \geq 7$. *$0.01 \leq p < 0.05$; **$0.001 \leq p < 0.01$; ***$p < 0.001$

Figure 4. NICD3 inhibits osteoclastogenesis and promotes osteoblastogenesis. (**A-C**) Expression of mouse-specific mRNA from tibiae of mice injected with PC3-NICD3 cells and treated with sucrose (Suc) or doxycycline (Dox): (**A**) IL-10, (**B**) OPG/RANKL ratio, and (**C**) bone sialoprotein (BSP), alkaline phosphatase (ALP), or osteocalcin (OCN). (**D-G**) Primary osteoblasts differentiated in the presence of conditioned medium (CM) from PC3-NICD3 cells treated with doxycycline (Dox) or vehicle (Ctrl). Colonies were stained for (**D**) ALP or crystal violet (CV). (**E**) Expression of mouse-specific mRNA from treated osteoblast cultures: osterix (OX), bone sialoprotein (BSP), or osteocalcin (OCN). (**F**) MTT assay of treated osteoblast cultures. (**G**) Levels of Cyclin A, D, E and tubulin (Tub) from treated osteoblast cultures assessed by immunoblotting. (**H-I**) Primary osteoclasts differentiated in the presence of conditioned medium (CM) from doxycycline (Dox) or vehicle-treated (Ctrl) PC3-NICD3 cells. (**H**) TRAP+ cells with $2 \geq$ nuclei quantified. (**I**) Expression of mouse-specific mRNA from osteoclast cultures: MM9, cathepsin K (CathK), calcitonin receptor (CR), or DC-Stamp. (**J**-**L**) Primary osteoclasts differentiated in the presence of conditioned medium (CM) from (**J**) 22Rv1-shN3 (Notch3 shRNA), (**K**) C42B-shN3, and (**L**) C4-2B-NICD3 expressing cells.

Percentage of TRAP+ cells quantified. Error bars are S.E.M, n=3. *0.01≤p<0.05; **0.001≤p<0.01; ***p<0.001

Figure 5. Notch3 promotes osteoblastic lesion development in an MMP3-dependent manner. (**A**) Primary osteoclasts differentiated in the presence of 25 ng/ml recombinant human MMP-3 (rMMP3). Percentage of TRAP+ cells with 2 ≥ nuclei quantified. (**B-C**) Primary osteoblasts differentiated in the presence of recombinant MMP3 (rMMP3) (**B**) immunostained for ALP or (**C**) proliferation measured by MTT assay. (**D-F**) Tet-inducible PC3-NICD3 cells were engineered to stably express MMP-33 shRNA (PC3-NICD3-shMMP3). (**D**) Primary osteoclasts or (**E**) primary osteoblasts differentiated in the presence of conditioned medium (CM) from doxycycline-treated (Dox) or vehicle-treated (Ctrl) PC3-NICD3 or PC3-NICD3-shMMP3 cells. (**D**) Percentage of TRAP+ cells quantified. (**E**) MTT assay of treated osteoblasts. (**F**) Tet-inducible PC3-NICD3 and PC3-NICD3-shMMP3 injected into tibiae of mice treated with doxycycline (Dox) or sucrose (Suc). Lytic lesion area on X-ray quantified. (**G**) Tibiae stained with H&E, anti-Notch3, or anti-MMP-3. Error bars are S.E.M, n≥8. *0.01≤ p<0.05; **0.001≤p<0.01; ***p<0.001

Figure 6. Notch3 and MMP-3 expression are higher in bone metastases relative to visceral metastasis. Tissue microarrays, (**A**) TMA-170 and (**B**) UWTMA79 probed for Notch3 and MMP-3 expression by IHC. Levels of expression were compared between patient-matched visceral and bone metastases. (**C**) Frequency of Notch3 and MMP-3 co-expression across all samples.

FIGURE 1

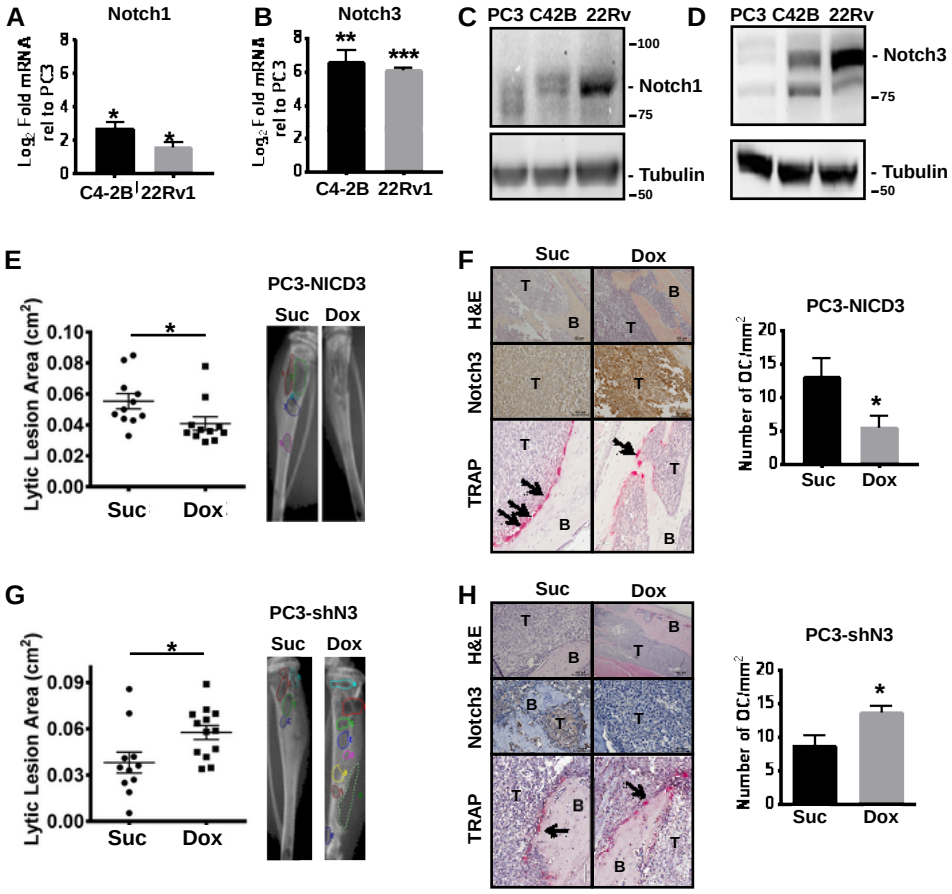

FIGURE 2

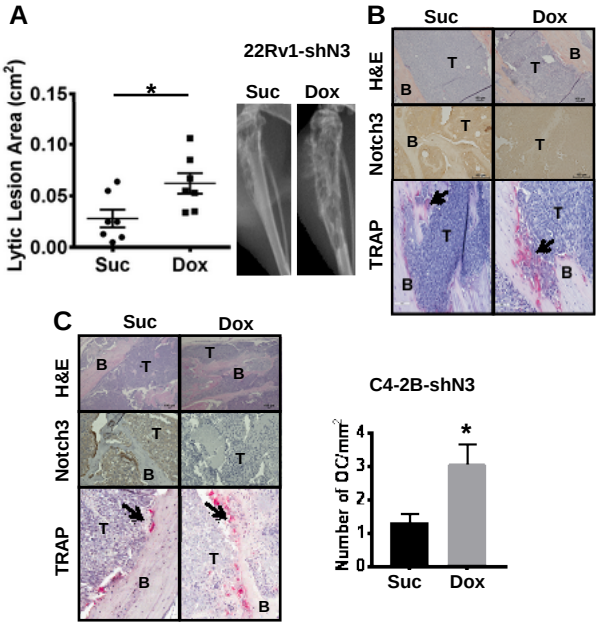

FIGURE 3

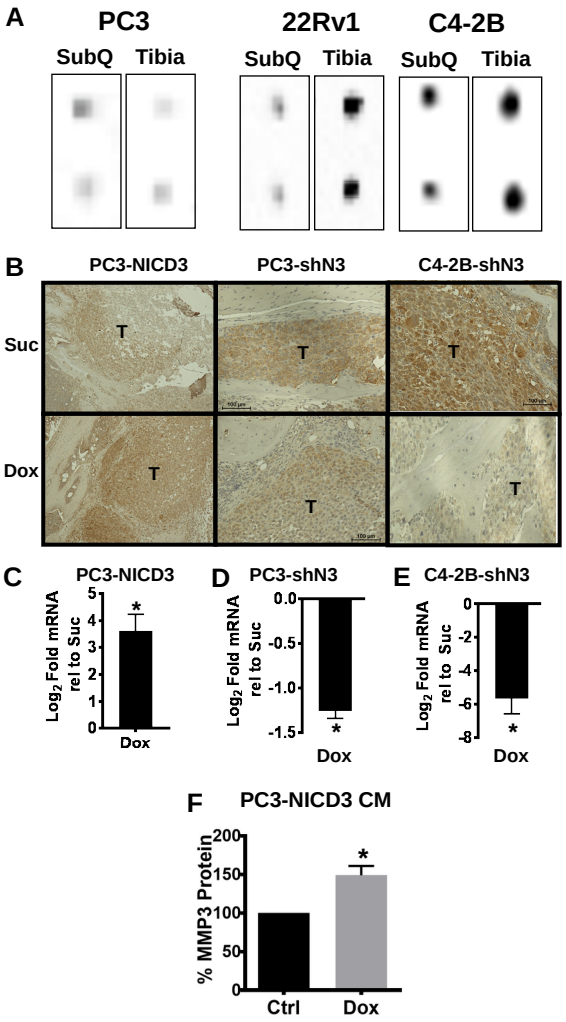

FIGURE 4

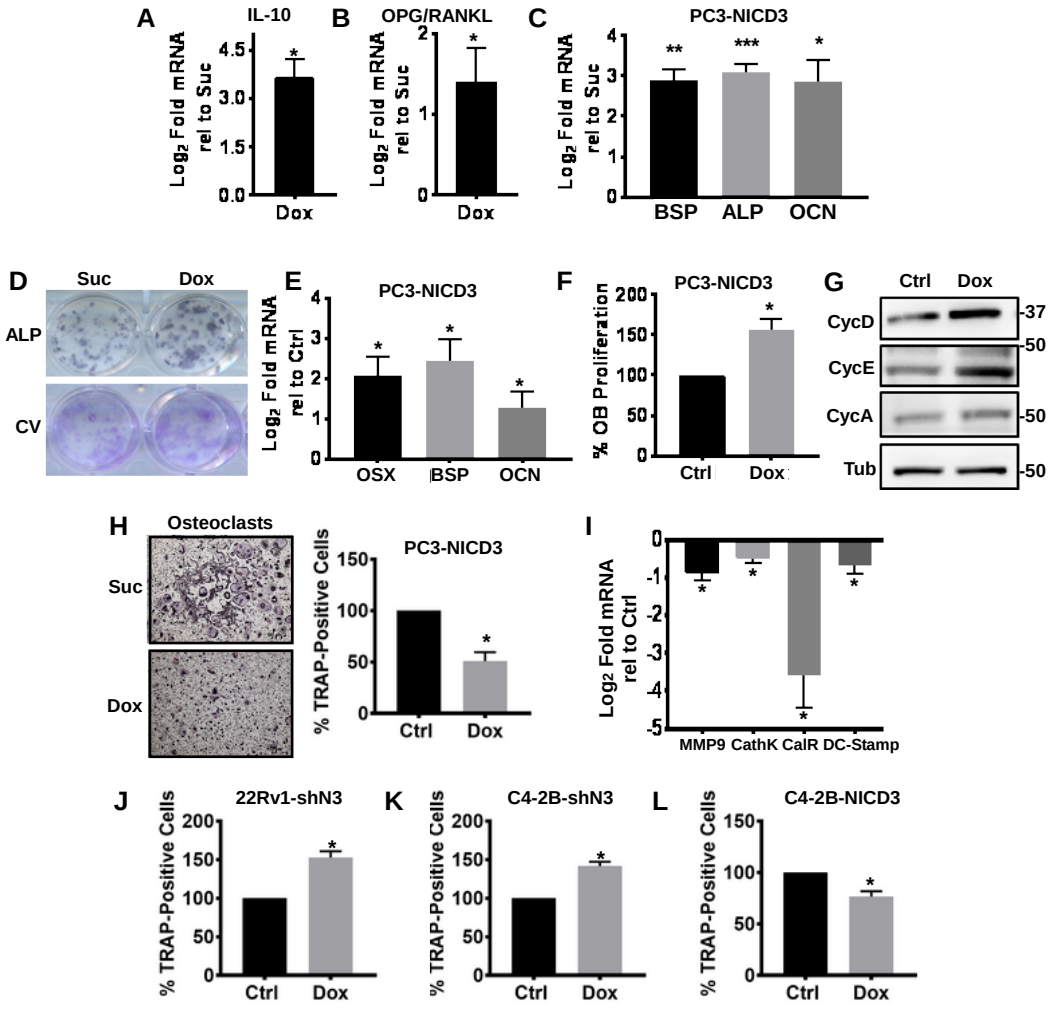

FIGURE 5

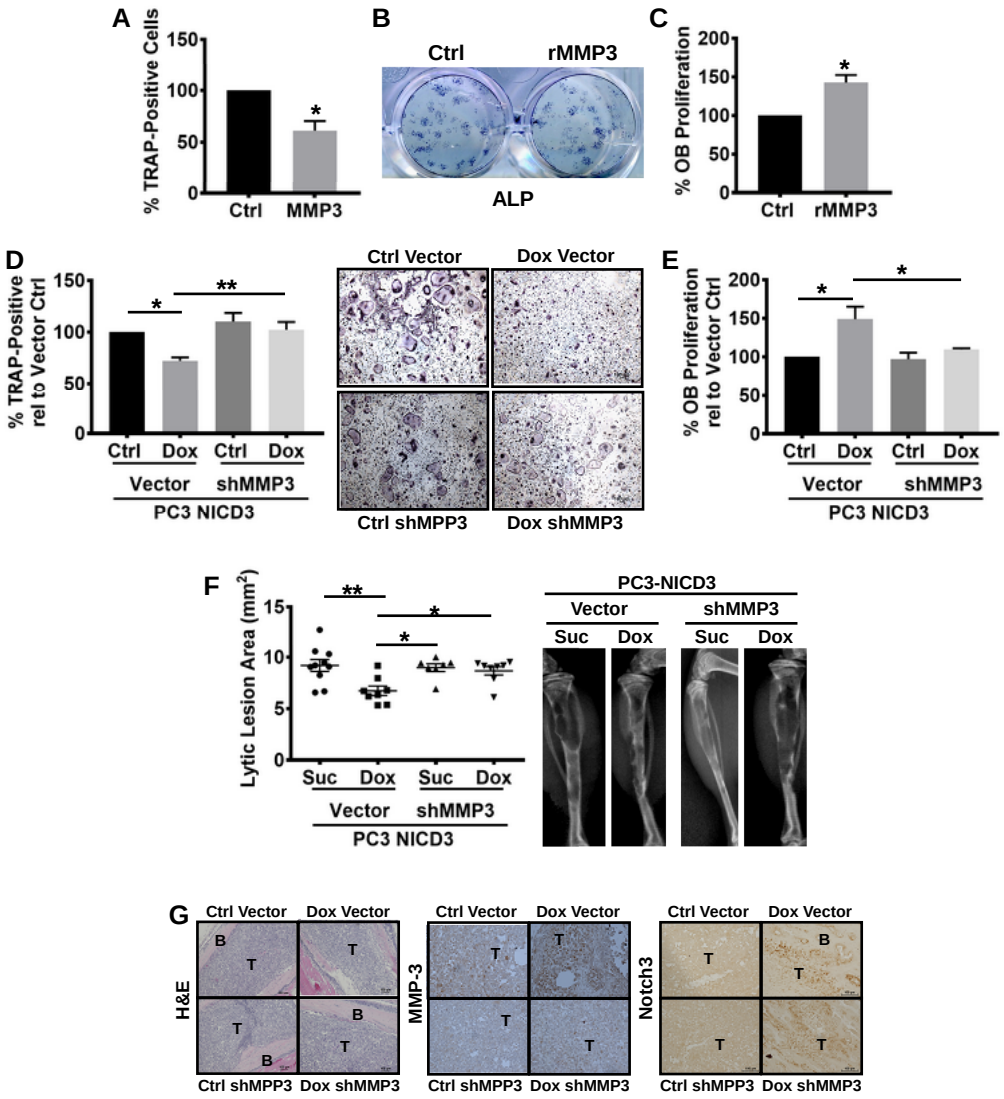

FIGURE 6

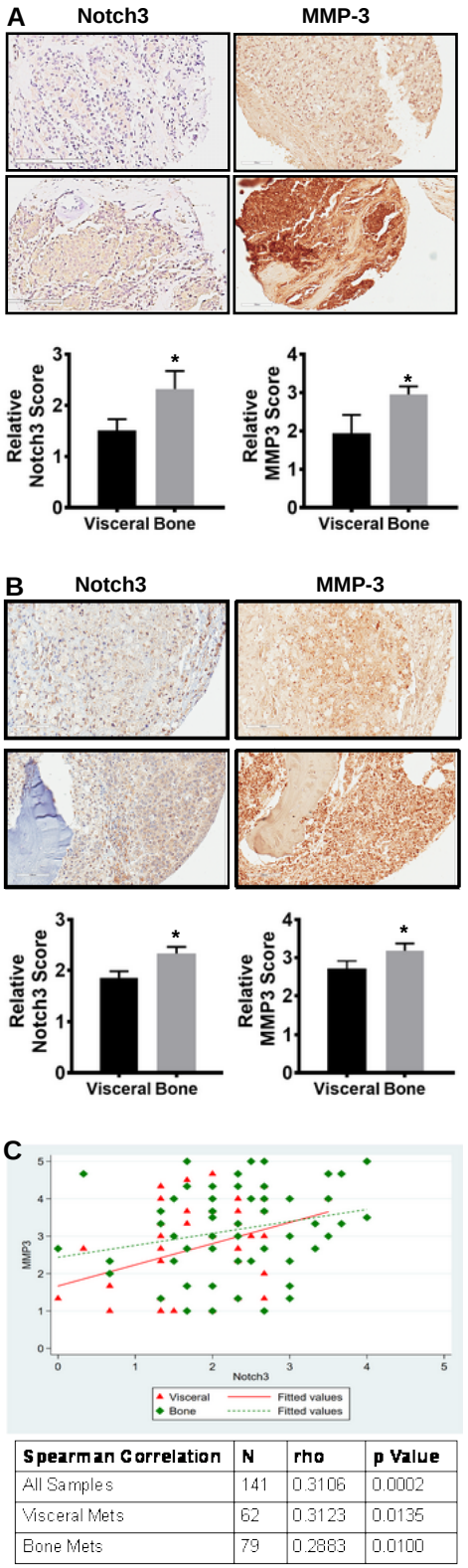

Spearman Correlation	N	rho	p Value
All Samples	141	0.3106	0.0002
Visceral Mets	62	0.3123	0.0135
Bone Mets	79	0.2883	0.0100